Proceedings of the LHCP2015 Conference, St. Petersburg, Russia, August 31 - September 5, 2015

Editors: V.T. Kim and D.E. Sosnov

Searches for Neutral 2HDM, MSSM and NMSSM Higgs Bosons at the LHC

MATTHIAS SCHRÖDER

KIT — Karlsruher Institut für Technologie
Institut für Experimentelle Kernphysik
Hermann-von-Helmholtz-Platz 1, 76344 Eggenstein-Leopoldshafen, Germany

matthias.schroeder@kit.edu

On behalf of the ATLAS and CMS Collaborations

Abstract. After a Higgs boson with a mass of 125 GeV has been discovered, it is still unclear whether this is the Higgs boson of the Standard Model or whether it is part of an extended Higgs sector, which is predicted by various models of new physics such as the minimal supersymmetric extension to the Standard Model. Recent results of direct searches for additional, neutral Higgs bosons by the ATLAS and CMS experiments are reviewed, which are based on pp collision data collected at centre-of-mass energies of 7 and 8 TeV corresponding to integrated luminosities of approximately 5 and 20 fb^{-1}, respectively.

Introduction

While the Higgs boson with a mass of 125 GeV [1] is consistent with the Standard Model (SM) expectations, non-SM couplings are only excluded up to branching ratios of $\approx 30\%$ with the current data [2]. Furthermore, numerous beyond-the-SM (BSM) models predict extended Higgs sectors, which may contain a SM-like Higgs boson.

Their phenomenology is described generically in Two-Higgs-Doublet-Models (2HDMs), which are effective extensions to the SM that add another Higgs doublet [3]. After electroweak symmetry breaking, five physical states remain: a light and a heavy CP-even boson h and H, an CP-odd boson A, all of which are neutral and collectively denoted ϕ, and two charged bosons $\text{H}^{\pm}$. The light state h is typically identified with the 125 GeV Higgs boson. If in addition the non-existence of flavour-changing neutral currents is imposed, the 2HDMs are defined by six free parameters: the masses m_{H}, m_{A}, $m_{\text{H}^{\pm}}$ of the additional Higgs bosons, the ratio $\tan\beta$ of the vacuum expectation values of the two doublets, and the mixing angle α of the two CP-even states h and H. Different types of 2HDMs are distinguished, depending on their Yukawa-coupling structure. For this article, type-II models are of interest, where one Higgs doublet couples to the up-type and the other to the down-type fermions.

The minimal supersymmetric extension to the SM (MSSM) is an example of a concrete model whose Higgs sector is described by a type-II 2HDM. In this case, however, the supersymmetry poses additional constraints on the Higgs sector, which, at tree level, is then completely defined by two parameters, conventionally chosen as m_{A} and $\tan\beta$ [4].

Other models feature more complex Higgs sectors, such as the Next-to-MSSM (NMSSM), which introduces an additional singlet field resulting in seven physical Higgs bosons. The light bosons can have masses below 125 GeV without violating the experimental constraints if their singlet component is large enough. The NMSSM is theoretically appealing because it solves the small fine-tuning problem introduced in the MSSM by the $m_{\text{h}} = 125$ GeV requirement [5].

In this article, recent results of direct searches for additional Higgs bosons performed by the ATLAS and CMS experiments [6, 7] at the LHC are reviewed, focusing on searches for neutral Higgs bosons as predicted in the MSSM, the 2HDMs, and the NMSSM. The analyses are performed with 4.9 and 19.7 fb^{-1} of pp collision data collected at centre-of-mass energies of 7 and 8 TeV, respectively.

Searches for Heavy Neutral MSSM Higgs Bosons

The heavy neutral MSSM Higgs bosons H and A are expected to be predominantly produced either in gluon-gluon fusion (ggF) or b-quark associated (bA) production at the LHC. Since the Yukawa-coupling to down-type fermions is enhanced by $\tan^2\beta$ relative to the SM over the whole m_A range, the latter production mode dominates for not-too-small values of $\tan\beta$ above approximately 10. Likewise, the branching fractions ($\mathcal{B}$) to charged leptons and down-type fermions are enhanced [8]. Searches performed by ATLAS and CMS probe all relevant and experimentally accessible channels $b\bar{b}$, $\tau\tau$, and $\mu\mu$.

CMS has performed a search for $\phi \to b\bar{b}$ using the $19.7\,\text{fb}^{-1}$ of 8 TeV data [9]. With a branching ratio of often up to 90%, this channel has the by far largest production rate but suffers from an overwhelming QCD-multijet background. Events are therefore selected by requiring the three leading jets (the three jets with highest transverse momentum p_T) to be identified as initiated by b-quarks (b-tagged). This selection targets at the typically dominant bA signal-production and largely reduces the QCD-multijet contribution. In order to cope with the huge event rate, dedicated triggers have been developed that perform online b-tagging. The signal is expected to manifest as a single resonance in the invariant-mass distribution m_{12} of the leading two jets, which is caused by the degenerate contributions of the A and H bosons. The remaining SM background consists almost entirely of QCD-multijet events with three real b jets or with two b jets and one mis-tagged light-flavour jet, leading to a non-resonant m_{12} distribution determined by the trigger turn-on and multijet production cross-section. The background is determined with a data-driven procedure, fitting a superposition of templates for each of the different flavour combinations of the three leading jets to the data. The template shapes are derived from a data control-sample of events with two b-tagged jets, which are weighted by the b-tag probability of the un-tagged jet.

The observed data are well described by the background-only expectation. In absence of a signal, model-independent upper limits are derived on the resonance production rate $\sigma(pp \to b\phi + X) \times \mathcal{B}(\phi \to b\bar{b})$, which range from 250 to 1 pb for signal-mass hypotheses from 100 to 900 GeV, respectively. The results, combined with the results of a previous analysis based on 7 TeV data [10], are also interpreted as constraints on the MSSM parameters, expressed as limits at 95% confidence level (C. L.) in $(\tan\beta, m_A)$ space. The other MSSM parameters are chosen to be fixed at certain benchmark values, where in addition to the traditionally used m_h^{max} benchmark scenario also several other recently proposed scenarios are considered, that are compatible with either h or H having a mass of 125 GeV in most parts of the parameter space [11]. This is not the case in the m_h^{max} scenario, which is therefore disfavoured by the data. The sensitivity in the $m_h^{\text{mod+}}$ scenario, for example, reaches up to $m_A = 500$ GeV and down to $\tan\beta = 14$ at low m_A, cf. Fig. 1 (left). The $\phi \to b\bar{b}$ channel is expected to be particularly sensitive to the higgsino-mass parameter μ of the MSSM [11]. This is evident in Fig. 1 (right), where the limit is compared for different values of μ, varying from $\tan\beta = 30$ for $\mu = -500$ GeV to beyond 60 for $\mu = +500$ GeV at $m_A = 500$ GeV.

Both ATLAS and CMS have performed searches in the $\phi \to \tau\tau$ channel, which contributes with $\mathcal{B} \approx 10\%$ [13, 14, 15]. The analyses deploy data at 7 and 8 TeV, and up to five $\tau\tau$ final-states — $e\tau_h$, $e\mu$, $\mu\tau_h$, $\mu\mu$, and $\tau_h\tau_h$ — are considered. Events are generally selected by requiring two oppositely charged, well isolated leptons. Additional, channel-dependent selection criteria are applied to suppress contributions from SM background processes; for example, in the $\mu\tau_h$ channel the transverse mass of the μ and the missing transverse momentum ($\not{E}_T$) is restricted to reject W+jets events. Depending on the analysis, the selected events are categorised according to the number of b-tagged jets, the τ-p_T, the employed trigger selection, and the signal-mass hypothesis in order to enhance the sensitivity and to distinguish between the different production modes. The invariant mass of the di-τ system is reconstructed using different estimators that are based on the leptons and on the $\not{E}_T$ to infer the neutrino momenta, which results into a relative mass resolution of typically 20% at 100 GeV. One of the dominant SM background contributions arises from $Z \to \tau\tau$ events; where important, it is determined from data with an embedding technique, in which the muons in $Z \to \mu\mu$ events are replaced by simulated τ-decay products. Further important backgrounds are due to W+jets and QCD-multijet events with jets mis-identified as τ_h and μ and are estimated from signal-depleted control regions in data.

In all channels, the observed data agree well with the SM-only expectation. Thus, model-independent upper limits on the resonance production rates $\sigma(pp \to \phi + X) \times \mathcal{B}(\phi \to \tau\tau)$ for the different production modes as well as limits on the MSSM parameters $\tan\beta$ and m_A are derived. The limits in the $m_h^{\text{mod+}}$ scenario obtained by CMS are shown in Fig. 1 (left); they reach up to $m_A = 1$ TeV (the plot shows only the range up to $m_A = 500$ GeV for better readability) and down to $\tan\beta = 5$ at low m_A. In this channel, sensitivity is reached also to the h state at 125 GeV, and therefore, the signal hypothesis is tested against a background plus SM-Higgs hypothesis. A similar result is obtained by ATLAS [14].

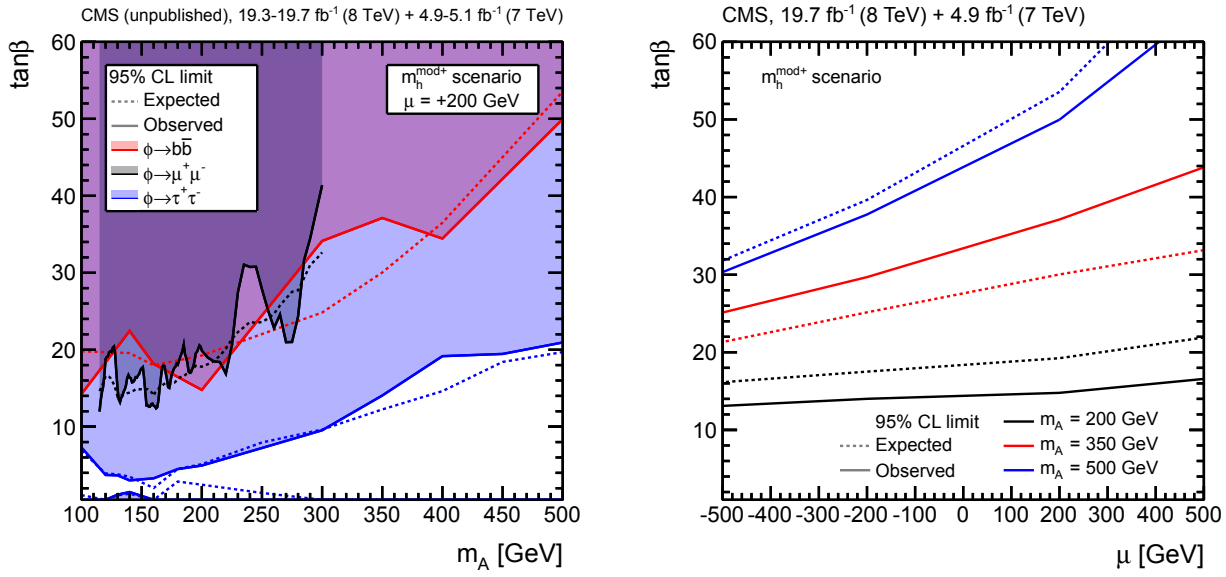

FIGURE 1. Expected (dashed lines) and observed (solid lines) upper limits at 95% C. L. on the MSSM parameter $\tan\beta$ in the $m_h^{\text{mod+}}$ benchmark scenario. Shown is (left) a comparison of the $\tan\beta$ limits versus m_A obtained in different final states $b\bar{b}$ [9], $\mu\mu$ [12], and $\tau\tau$ [13], with $\mu = +200$ GeV. The excluded parameter space (observed limit) is indicated by the shaded areas. The limit in the $\tau\tau$ final state extends to $m_A = 1$ TeV but is shown here only up to 500 GeV for better readability. Also shown (right) is a comparison of the $\tan\beta$ limits versus the higgsino-mass parameter μ obtained for three different values of m_A in the $b\bar{b}$ final state [9].

CMS has also performed a search in the di-μ final state using the 25 fb^{-1} of data at 7 and 8 TeV [12]; ATLAS has performed a similar search with 7 TeV data [16]. Although the branching fraction of this channel is below 10^{-3}, it benefits from the excellent relative mass resolution of approximately 1% at 125 GeV. Events are selected requiring two oppositely charged, well isolated muons. In order to suppress the $t\bar{t}$ background, events with $\not{E}_T > 35$ GeV and two or more b-tagged jets are rejected. The selected events are further categorised into events with one or zero b-tagged jets to enhance the sensitivity to the bA and ggF production processes, respectively. The di-μ invariant mass spectrum of the SM-background processes, which are dominated by Drell-Yan production, is modelled with an analytic function. The signal is expected to manifest as narrow resonances, which are parametrized by Voigt profiles, the shape of which are determined from simulation. In case of the MSSM interpretation, the signal model consists of two narrow resonances, one due to the h and the second one due to the degenerate A and H contributions, and their relative normalisation is fixed according to the choice of m_A and $\tan\beta$. The signal yield is extracted from fitting a linear combination of the signal and background models to the data.

No evidence of a signal is found, and the results are expressed as model-independent upper limits on $\sigma(pp \to \phi + X) \times \mathcal{B}(\phi \to \mu\mu)$ for the different production modes as well as on the MSSM parameters $\tan\beta$ and m_A in different benchmark scenarios. In the $m_h^{\text{mod+}}$ scenario, the exclusion at 95% C. L. on $\tan\beta$ reaches as low as 15 in the low-m_A region and to above 30 at m_A =300 GeV, cf. Fig. 1 (left).

As evident from Fig. 1 (left), the reviewed analyses probe the MSSM Higgs sector in different channels and complement each other. The most stringent limits arise from the $\tau\tau$ channel; the sensitivity in $\tan\beta$ is similar in the $b\bar{b}$ and $\mu\mu$ channels, where $\mu\mu$ has the lowest reach in m_A. The mass resolution is best in the $\mu\mu$ and worst in the $\tau\tau$ channel.

Searches for Pseudoscalar Higgs Bosons in 2HDMs

In most 2HDMs, the decay $A \to Zh$ of the pseudoscalar Higgs boson A into a Z boson and the Higgs boson at 125 GeV often has a large branching fraction for masses m_A above the kinematic threshold up to where the decay into two top quarks opens up and even beyond. In the MSSM, this is the case for low values of $\tan\beta$ [17].

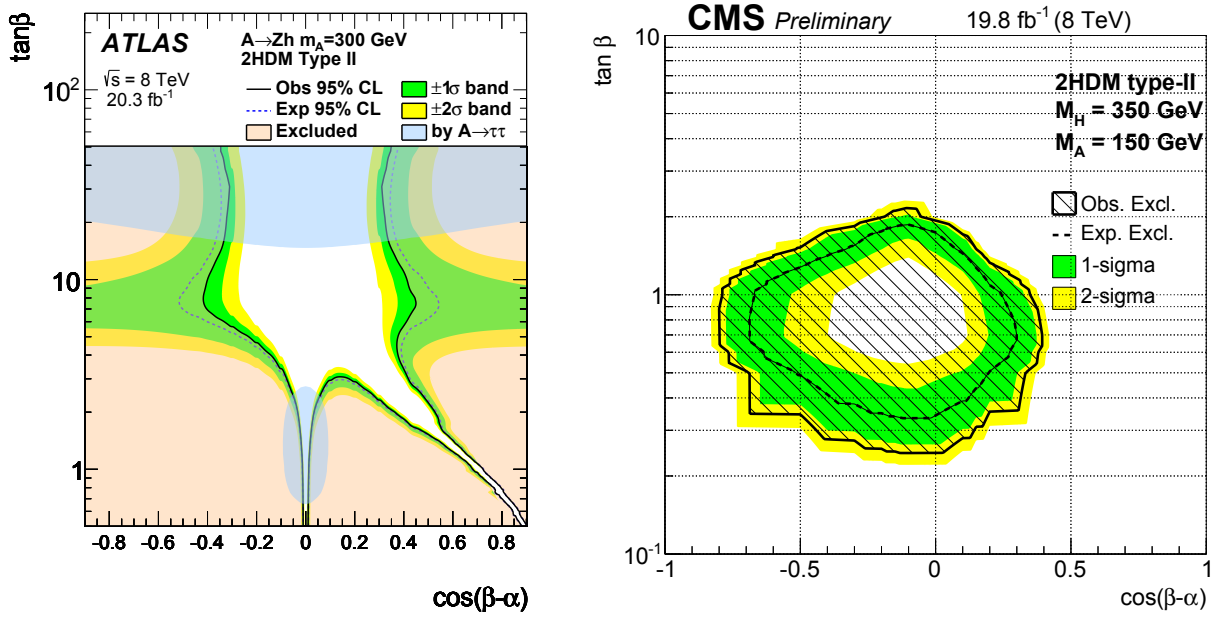

FIGURE 2. Expected (dashed lines) and observed (solid lines) limits at 95% C. L. on the parameters $\tan\beta$ and $\cos(\beta-\alpha)$ of the type-II 2HDM obtained for $m_{\mathrm{A}} = m_{\mathrm{H}} = m_{\mathrm{H}^{\pm}} = 300\,\mathrm{GeV}$ by the $\mathrm{A} \to \mathrm{Zh}$ search [18] (left) and for $m_{\mathrm{A}} = 150\,\mathrm{GeV}$, $m_{\mathrm{H}} = m_{\mathrm{H}^{\pm}} = 350\,\mathrm{GeV}$ by the $\mathrm{H} \to \mathrm{ZA}$ search [20] (right). Excluded regions (observed limit) are marked by the light shaded (left) and hatched (right) areas; the dark shaded area (left) shows the exclusion obtained by a reinterpretation of the $\phi \to \tau\tau$ search described in the text [14].

Both ATLAS and CMS have performed searches for A-boson production in ggF with $\mathrm{A} \to \mathrm{Zh}$ in final states where the Z boson decays into two electrons or muons and the h boson into two b quarks or tau leptons, using the $20\,\mathrm{fb}^{-1}$ of data collected at 8 TeV [18, 19, 20]. The leptonic Z decay offers a clean signature for triggering, while the $\mathrm{h} \to \mathrm{b\bar{b}}/\tau\tau$ rate is typically high. ATLAS also considers the $\mathrm{Z} \to \nu\nu$ decay, which improves the sensitivity at high signal masses. A peak search is performed in the invariant-mass spectrum of the two leptons and b quarks/τ leptons, and the mass resolution is improved by deploying a constraint of 125 GeV on the di-b-jet/di-τ mass in the reconstruction. Different additional procedures are performed to improve the signal-to-background discrimination. For example, CMS employs the output of a boosted-decision tree classifier that takes into account b-tagging and angular information of the Z decay products. Important SM backgrounds arise from Z+jets and $\mathrm{t\bar{t}}$ production and are determined from different control regions in data.

In the absence of a signal, the results are interpreted as constraints on the parameters of different 2HDMs, expressed as limits at 95% C. L. in $(\tan\beta, \cos(\beta-\alpha))$ space. Small contributions to the expected signal from bA production together with the combinatorics due to additional b jets are taken into account in the limit setting procedure. The limits obtained by ATLAS in the type-II 2HDM for $m_{\mathrm{A}} = m_{\mathrm{H}} = m_{\mathrm{H}^{\pm}} = 300\,\mathrm{GeV}$ are shown in Fig. 2 (left). Large parts of the parameter space are excluded, also at high values of $\tan\beta$. The sensitivity is reduced in the 'alignment limit' at $\cos(\beta-\alpha) \to 0$, where the h boson becomes SM like and the branching fraction $\mathcal{B}(\mathrm{A} \to \mathrm{Zh})$ vanishes, as well as in a narrow region in phase space towards $\cos(\beta-\alpha) = 1$ at small $\tan\beta$, where $\mathcal{B}(\mathrm{h} \to \mathrm{b\bar{b}}/\tau\tau)$ becomes small. Sensitivity to the region of the alignment limit is to some extent obtained by a reinterpretation of the results of the MSSM $\phi \to \tau\tau$ search [14] described above, as indicated in the figure. CMS has found similar limits.

Access to the interesting region of the alignment limit is also gained with a complementary analysis by CMS, where the light Higgs boson at 125 GeV is not explicitly required in the final state [20]. Instead, a search for $\mathrm{A/H} \to \mathrm{ZH/A}$ events is conducted, and either mass hierarchy of the heavy Higgs bosons A and H is considered in the interpretation. The resulting limits on the type-II 2HDM parameters $\tan\beta$ and $\cos(\beta-\alpha)$ are shown in Fig. 2 (right) for $m_{\mathrm{A}} = 150\,\mathrm{GeV}$ and $m_{\mathrm{H}} = m_{\mathrm{H}^{\pm}} = 350\,\mathrm{GeV}$.

Searches for Light Pseudoscalar NMSSM Higgs Bosons

The lightest pseudoscalar Higgs boson a of the NMSSM can have masses below 125 GeV without violating the experimental constraints by the SM Higgs-boson searches [5]. ATLAS has performed two searches for the decay $H \to aa$, where H is assumed to be either the 125 GeV boson or a second CP-even state, which is dominantly produced in ggF. Both searches employ 20.3 fb^{-1} of pp collision data collected at 8 TeV.

The first analysis targets events where one a boson decays to two muons and the other to two τ leptons, one of which decays leptonically [21]. It is assumed that the a boson only decays via the $\mu\mu$ or $\tau\tau$ channel. The search is performed for masses m_a of the a boson between 3.7 and 50 GeV with $m_H = 125$ GeV, and for different values of m_H between 100 and 500 GeV assuming $m_a = 5$ GeV. While the choice of the $m_a \to \mu\mu$ final-state leads to a low expected signal rate, it results in a high trigger efficiency, low signal-to-background ratio, and a narrow di-μ invariant mass resonance, which is used to identify a signal.

The two a bosons are expected to be produced back-to-back in the transverse plane with a high boost in most parts of the probed parameter space. Events are selected requiring two oppositely-charged, well-isolated muons constituting an $m_a \to \mu\mu$ candidate with $p_T > 40$ GeV. Further, an electron or muon well-separated in azimuth from the a candidate is required and there must be up to three additional tracks within a cone around the lepton, the leading of which has opposite charge to the lepton, which aims at reconstructing the $m_a \to \tau\tau$ decay. Additional isolation and quality criteria are imposed to suppress background events faking the τ signature. The expected signal di-μ mass distribution is modelled with a double-sided Crystal Ball (CB) function plus a Gaussian with different mean to describe small contributions due to $a \to \tau\tau \to \mu\mu + 4\nu$ decays. The SM background is dominated by Drell-Yan events and, at higher masses, $t\bar{t}$ events, which are parametrized essentially with exponential functions. Additional resonant contributions due to J/Ψ, Ψ', Υ_{1S}, Υ_{2S}, and Υ_{3S} mesons are modelled with CB functions, where the same mass-dependent resolution as for the signal model are assumed. The parameters of the signal and background model as well as the signal strength are determined in a simultaneous fit to the data in the signal region and in two background-enhanced control regions, which are selected by requiring the presence of additional light- or heavy-flavour jets in the events.

The data are well described by the background-only hypothesis. Thus, upper limits are set at 95% C. L. on the resonance production rate $\sigma(gg \to h) \times \mathcal{B}(h \to aa)$, which are shown in Fig. 3 (left) relative to the SM Higgs-boson ggF production rate as a function of m_a for $m_h = 125$ GeV. The result is scaled by $\mathcal{B}^2(a \to \tau\tau)$ to allow reinterpretation of the results given the $\mathcal{B}(a \to \tau\tau) + \mathcal{B}(a \to \mu\mu) = 1$ assumption.

The second analysis targets $H \to aa \to 4\gamma$ events where both a bosons decay into two photons [22]. The search

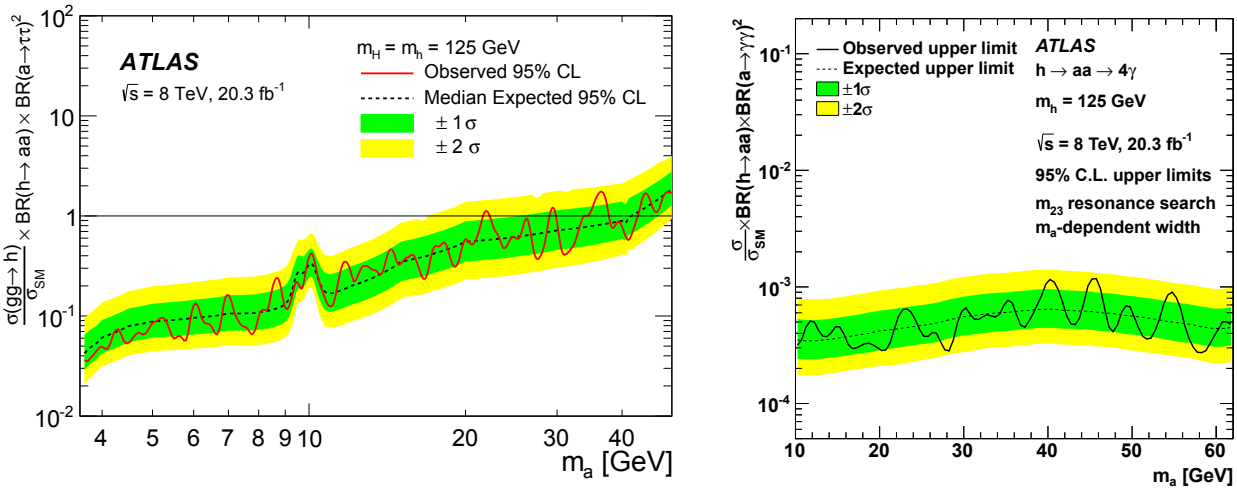

FIGURE 3. Observed (solid line) and expected (dashed line) upper limits on the $\sigma(gg \to h) \times \mathcal{B}(h \to aa)$ production relative to the SM Higgs-boson gluon-gluon fusion production rate as a function of m_a for $m_h = 125$ GeV. Shown are the results obtained in the $\mu\mu\tau\tau$ (left) and 4γ (right) final states, which are scaled by the appropriate branching fractions of the a boson final-states [21, 22]. The former limit is scaled by $\mathcal{B}^2(a \to \tau\tau)$ to account for the assumed branching ratios and allow reinterpretation of the results.

is performed for masses m_a of the a boson between 10 and 62 GeV with $m_H = 125$ GeV, and also for larger values of m_H with an adjusted m_a range up to the kinematic threshold.

Events are selected requiring at least three isolated photons, which provides sensitivity also to other BSM processes such as $Z \to \gamma a(\gamma\gamma)$ and rare SM processes such as $Z \to 3\gamma$. A resonance search is performed in the two-photon invariant mass distribution m_{23} of the second and third highest-p_T photons, which results in the best sensitivity to the $H \to aa \to 4\gamma$ process. The signal is modelled with a Gaussian. The dominant background arises from rare SM processes with three or more prompt photons as well as processes including electrons or jets misidentified as photons. It is determined from data with a fit in m_{23} side-band regions, where the background distributions is modelled by a fourth-order polynomial.

The observed data is well described by the background-only hypothesis, and thus, upper limits are set at 95% C. L. on the resonance production rate $\sigma(gg \to h) \times \mathcal{B}(h \to aa) \times \mathcal{B}^2(a \to \gamma\gamma)$. They are shown in Fig. 3 (right) relative to the SM Higgs-boson ggF production rate as a function of m_a for $m_h = 125$ GeV.

Conclusions

ATLAS and CMS have performed a wide variety of searches for additional Higgs bosons. In this article, recent searches for neutral Higgs bosons as predicted by the MSSM, 2HDMs, and NMSSM have been discussed, which have been performed with up to 25 fb^{-1} of 7 and 8 TeV data. No significant deviation from the SM is observed, and the results are used to derive stringent, complementary constraints on the BSM-Higgs parameter space.

REFERENCES

[1] ATLAS and CMS Collaborations, Phys. Rev. Lett. **114**, p. 191803 (2015), arXiv:1503.07589 [hep-ex] .
[2] ATLAS and CMS Collaborations, (2015), ATLAS-CONF-2015-044, CMS-PAS-HIG-15-002 .
[3] G. C. Branco et al., Phys. Rept. **516**, 1–102 (2012), arXiv:1106.0034 [hep-ph] .
[4] H. P. Nilles, Phys. Rept. **110**, 1–162 (1984).
[5] R. Dermisek and J. F. Gunion, Phys. Rev. **D76**, p. 095006 (2007), arXiv:0705.4387 [hep-ph] .
[6] ATLAS Collaboration, JINST **3**, p. S08003 (2008).
[7] CMS Collaboration, JINST **3**, p. S08004 (2008).
[8] LHC Higgs Cross Section Working Group, (2013), 10.5170/CERN-2013-004, arXiv:1307.1347 [hep-ph] .
[9] CMS Collaboration, JHEP **11**, p. 071 (2015), arXiv:1506.08329 [hep-ex] .
[10] CMS Collaboration, Phys. Lett. **B722**, 207–232 (2013), arXiv:1302.2892 [hep-ex] .
[11] M. S. Carena et al., Eur. Phys. J. **C73**, p. 2552 (2013), arXiv:1302.7033 [hep-ph] .
[12] CMS Collaboration, Phys. Lett. **B752**, 221–246 (2016), arXiv:1508.01437 [hep-ex] .
[13] CMS Collaboration, (2015), CMS-PAS-HIG-14-029 .
[14] ATLAS Collaboration, JHEP **11**, p. 056 (2014), arXiv:1409.6064 [hep-ex] .
[15] CMS Collaboration, JHEP **10**, p. 160 (2014), arXiv:1408.3316 [hep-ex] .
[16] ATLAS Collaboration, JHEP **02**, p. 095 (2013), arXiv:1211.6956 [hep-ex] .
[17] A. Djouadi and J. Quevillon, JHEP **10**, p. 028 (2013), arXiv:1304.1787 [hep-ph] .
[18] ATLAS Collaboration, Phys. Lett. **B744**, 163–183 (2015), arXiv:1502.04478 [hep-ex] .
[19] CMS Collaboration, Phys. Lett. **B748**, 221–243 (2015), arXiv:1504.04710 [hep-ex] .
[20] CMS Collaboration, submitted to Phys. Lett. B (2015), CMS-PAS-HIG-15-001 .
[21] ATLAS Collaboration, Phys. Rev. **D92**, p. 052002 (2015), arXiv:1505.01609 [hep-ex] .
[22] ATLAS Collaboration, submitted to EPJC (2015), arXiv:1509.05051 [hep-ex] .